Utah State University
DigitalCommons@USU

All Physics Faculty Publications | Physics

10-2003

Utilising Riometry to Observe Gravity Waves in the Sunlit Mesosphere

M. J. Jarvis

R. E. Hibbins

Michael J. Taylor
Utah State University

T. J. Rosenberg

Follow this and additional works at: http://digitalcommons.usu.edu/physics_facpub

Part of the Physics Commons

Recommended Citation
Jarvis, M.J., R. E. Hibbins, M.J. Taylor and T.J. Rosenberg, Utilising riometry to observe gravity waves in the sunlit mesosphere, J. Geophys. Res., 30, No. 19, 1979, doi:10.1029/ 2003GL017885, 2003.

This Article is brought to you for free and open access by the Physics at DigitalCommons@USU. It has been accepted for inclusion in All Physics Faculty Publications by an authorized administrator of DigitalCommons@USU. For more information, please contact dylan.burns@usu.edu.

Utilizing riometry to observe gravity waves in the sunlit mesosphere

M. J. Jarvis and R. E. Hibbins
British Antarctic Survey, Cambridge, UK

M. J. Taylor
Center for Atmospheric and Space Sciences, Utah State University, Logan, Utah, USA

T. J. Rosenberg
Institute for Physical Science and Technology, University of Maryland, College Park, Maryland, USA

Received 3 June 2003; revised 6 August 2003; accepted 25 August 2003; published 4 October 2003.

[1] The novel use of imaging riometers to observe mesospheric gravity waves is described. Imaging riometers respond to changes in the absorption of cosmic radio noise in the ionospheric D-region which enables them to detect the compression and rarefaction of the atmosphere at ~90 km altitude generated by the passage of gravity waves. A considerable advantage of this method is that, unlike conventional techniques which rely on imaging faint optical emissions from the airglow layer at ~87 km altitude, riometers remain operative under daylit, moonlit or cloudy conditions. This is particularly important for research into gravity wave forcing of mesospheric temperature at polar latitudes in summer when continuous 24-hour daylight prevails. An example in which the same wave event is characterized in co-located airglow imager and imaging riometer shows good agreement between the two instruments. *INDEX TERMS:* 0310 Atmospheric Composition and Structure: Airglow and aurora; 3332 Meteorology and Atmospheric Dynamics: Mesospheric dynamics; 3384 Meteorology and Atmospheric Dynamics: Waves and tides; 3394 Meteorology and Atmospheric Dynamics: Instruments and techniques; 2437 Ionosphere: Ionospheric dynamics. **Citation:** Jarvis, M. J., R. E. Hibbins, M. J. Taylor, and T. J. Rosenberg, Utilizing riometry to observe gravity waves in the sunlit mesosphere, *Geophys. Res. Lett.*, *30*(19), 1979, doi:10.1029/2003GL017885, 2003.

1. Introduction

[2] Observing and quantifying gravity waves in the polar mesosphere is an important pre-requisite both for understanding vertical energy transfer through the Earth's atmosphere and for incorporating the effects of mesospheric circulation and temperature into global circulation models. Gravity waves, propagating upwards from the troposphere, grow in amplitude due to the increasingly rarefied atmosphere and can eventually deposit their momentum in the mesosphere, forcing the zonal wind [*Lindzen*, 1981]. As a consequence of this forcing, the filtering of the waves by the stratospheric horizontal wind field through which they propagate, and the action of the Coriolis force, a meridional mesospheric wind flows from the summer to the winter pole. Air is driven upwards (downwards) at the summer (winter) pole and the consequent adiabatic cooling (heating) results in a summer mesopause temperature ~70K colder than radiative equilibrium would suggest. Much of the momentum flux comes from waves with periods of 30 minutes or less [*Fritts and Vincent*, 1987]; this forces the mean flow when non-acceleration conditions are violated [e.g., *Walterscheid*, 2001].

[3] The amplitude and direction of gravity waves in the mesosphere can be quantified from the ground by imaging optical emissions from airglow layers [*Taylor et al.*, 1995]. The airglow acts as a tracer for the rarefaction and compression of the atmosphere generated by the waves. However, the technique necessitates both darkness and cloudless conditions and thus it is not possible to observe short-period mesospheric gravity waves at polar latitudes during summer due to the continuous 24-hour daylight.

[4] This paper describes, for the first time, observations of mesospheric gravity waves using an imaging riometer. This technique uses fluctuations in ionospheric absorption as a tracer for the gravity waves and hence can be used during daylight. The study exploits the joint deployment and scientific collaboration between the British Antarctic Survey (BAS) and the University of Maryland regarding the imaging riometer at Halley Research Station (76°S, 27°W), Antarctica, and between BAS and Utah State University regarding a co-located airglow imager.

2. The Imaging Riometer

[5] Riometers exploit the fact that cosmic radio noise provides a background source outside the Earth's environment. As this radio noise propagates through the atmosphere to the Earth's surface it suffers absorption because the radio waves excite the ionised plasma of the ionosphere which then loses energy by collision with the neutral air. The riometer technique compares the strength of the cosmic radio noise signal received on the ground with its own long term sidereally-cyclic signal strength to determine the level of absorption at any moment of time [e.g., *Krishnaswamy et al.*, 1985]. At riometer frequencies (typically 30MHz) this absorption has a marked peak near 90 km where the product of the electron density and neutral density maximises. Riometers are primarily used to measure enhancement of the D-region ionosphere by energetic charged particle precipitation driven by magnetospheric electrodynamics [cf., *Stauning*, 1996].

[6] An advancement on the simple riometer is the imaging riometer [*Detrick and Rosenberg*, 1990] which utilises

Copyright 2003 by the American Geophysical Union.
0094-8276/03/2003GL017885

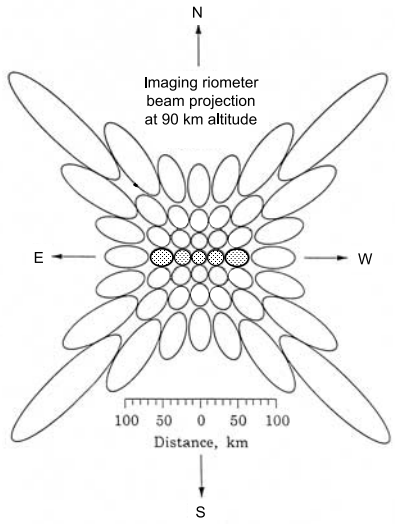

Figure 1. The projection of the imaging riometer beams onto a horizontal plane at 90 km altitude, as defined by their beam 3dB power contour [adapted from *Detrick and Rosenberg*, 1990]. The central east-west line of five beams discussed in the text are shaded.

an antenna array to generate several narrow receiving beams to spatially sample the D-region. The imaging riometer at Halley, Antarctica, operates on 38.2 MHz and samples an area some 240 km by 240 km with 49 beams every 1 s [*Rose et al.*, 2000]. Individual beams cover different areas because of the obliquity of their projection onto a horizontal layer as shown in Figure 1. Thus, the 3-dB projections of the beams near the centre are nearly circular with a diameter of approximately 20 km while those near the corners form a distorted ellipse with major and minor axes of ~110 km by ~40 km respectively.

3. Gravity Wave Observations

[7] When a gravity wave propagates through the mesosphere it will alternately compress and rarefy the atmosphere. Due to the rapid recombination time of D-region electron density enhancements, any increase or depletion in electron density as a direct result of these compressions and rarefactions is likely to persist only for a few seconds compared to the period, of several minutes, of the wave. However the neutral density modulations induced by the wave will induce spatial modulations both in the electron production rate and in the effective collision frequency between the neutrals and electrons. The D-region absorption, which is dependent upon the product of this collision frequency and the electron density, will thus be modulated by the wave and can be detected by the imaging riometer as a tracer for the wave. This principle has been demonstrated [*Fraser*, 1977] by the detection of five-day planetary wave oscillations in ionospheric absorption measured using an ionosonde but short period atmospheric gravity waves have not been reported in riometer data before.

[8] The observation of gravity waves using riometry is best demonstrated via an example where the same (necessarily night-time) wave event was observed using both an imaging riometer and a co-located airglow imager. Evidence of the wave event in the airglow imager was first observed at 07.25 UT in the form of patches of wave activity in different areas of the sky. By 07.49 UT wavefronts extended approximately north-south across the entire field-of-view and these persisted until 10.08 UT when dawn sunlight made further measurements impossible. Throughout the period between 07.49 UT and 10.08 UT the wavefront orientation and wavelength continued to show similar characteristics but were not always clearly visible over the entire field-of-view; different areas of the image showed more distinct wave images at different times and under different image brightness and contrast settings. Waves in the riometer data became significant around 08.00 UT and persisted until around 12.30 UT.

[9] Figure 2 shows an optical image of the OH airglow layer (~87 km altitude) over Halley on 7 June 2000 at 09.43:20 UT. Clearly visible are the signatures of gravity waves with their wavefronts running approximately up the page. The inset shows the boxed area of the original image with the star-field computationally removed and the resulting image median-smoothed. By analysing this selected wave structure over a time series of images it is possible to determine the wave parameters. Figure 3 shows the airglow intensity at approximately two-minute intervals, measured along a line perpendicular to the wavefronts in the Figure 2 inset. The eastward motion of the waves with time is clearly apparent. From cross-correlation between these sequences the horizontal wave parameters can be derived. The wave was estimated to have a mean wavelength λ of 16 ± 2 km, to travel with a velocity relative to the observer c_{obs} of 24 ± 3 ms^{-1}, to have a directional bearing of travel towards 70° and to exhibit a peak-to-peak intensity to mean intensity ratio $\Delta I/I$ of 6 ± 2%. The error limits cover wave periods between 10 and 14 minutes.

[10] Figure 4 shows the ionospheric absorption measured during the same wave event in the five most central beams aligned along the east-west direction of the co-located imaging riometer. These five beams are shaded in Figure 1;

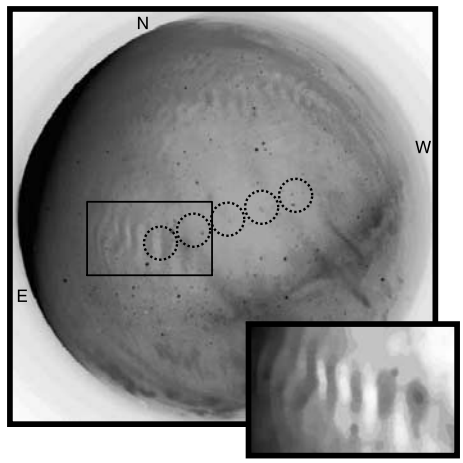

Figure 2. The unprocessed image of OH airglow (~87 km altitude) over Halley, Antarctica, at 09.43:20 U.T. on 7 June 2000. The circles show the spatial extent of the riometer beams shaded in Figure 1 projected to 87 km. The inset shows the gravity wave event clearly in an enhanced section from that image.

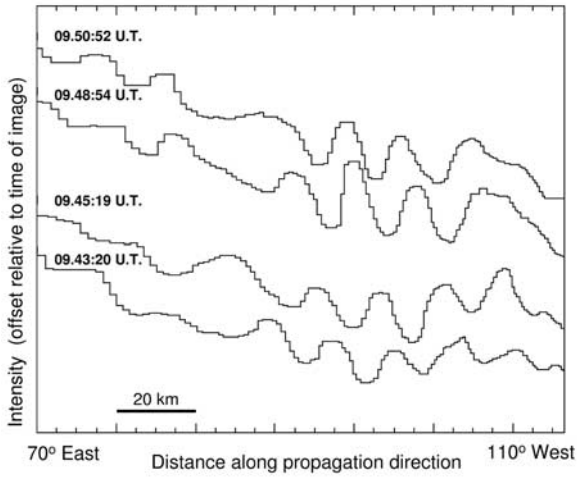

Figure 3. Stack plot of airglow intensity measured along a line perpendicular to the phase fronts from a sequence of four consecutive images. The eastward movement of the phase front is clear.

note that both the airglow image and the imaging riometer beam pattern are viewed as if looking upwards toward the sky so that bearings rotate anticlockwise from north. Wave signatures can particularly be seen in the three most eastward beams. These beams correspond to the region of the sky where clearly defined gravity wave signatures are present in the airglow (Figure 2). Sunrise at 87 km altitude occurred overhead at 11.45 UT but sunlight rendered airglow observations impossible from ~10.10 UT after which wave signatures continued to be observed by the riometer, particularly in the central and east-of-central beams.

4. Discussion

[11] Radio wave absorption measured by the riometer technique is proportional to $N\nu$, where N is the electron concentration and ν is the effective electron collision frequency. In turn, ν is approximately proportional to $n.T^{1/2}$ (where n is the neutral density and T is temperature) up to 100 km altitude where neutrals dominate. *Swenson and Gardner* [1998] modelled the gravity wave induced perturbations in mesospheric airglow and temperature using analytical models. They demonstrated that, for gravity waves with a vertical wavelength in excess of 15 km, the 6% peak-to-peak OH intensity oscillation observed for this event might typically be associated with a sodium abundance variation of ~10%. *Hickey and Plane* [1995] have shown that sodium can be treated as a passive dynamical tracer above 85 km. Thus, assuming the gravity wave temperature and density perturbations are anti-correlated with the same relative magnitude [*Swenson and Gardner*, 1998], the 6% peak-to-peak airglow intensity variation observed might be associated with a peak-to-peak absorption variation in the region of 7%. The perturbations in absorption observed for this event (Figure 4) occur against a mean background absorption level of approximately 0.13 dB. Thus a 7% variation in absorption would be approximately 0.009 dB. If the electron production rate is also modulated by the neutral density variation then the absorption variation may be several percent higher than this. The observed oscillations vary between ~0.01 and 0.03 dB, in good agreement with this expectation.

[12] A statistical study of many rocket measurements [*Baker and Stair*, 1988] shows the OH airglow layer mean altitude to be 87 ± 3 km with a layer thickness of 9 ± 3 km. The altitude of the riometer observations is largely dependent upon the causative mechanism for the prevailing vertical electron concentration profile. An altitude of 90 km is usually quoted for the maximum absorption detected by riometer absorption. Here, however, the instrument is not being used for the more normal substorm precipitation studies and therefore the peak absorption altitude is likely to be different.

[13] Data bases of wide-beam 27.6 MHz riometer absorption and night-time rocket-based electron concentration profiles from northern Scandinavia have been combined [*Friedrich and Torkar*, 1983] to generate typical absorption altitude profiles pertaining to different levels of riometer absorption. These showed that when riometer absorption was above ~0.5 dB, then the altitude of the peak was ~86 km and two thirds of the absorption integrated along the path occurred in a 17 km altitude range from ~78 km to ~95 km. As absorption decreased from ~0.5 dB to 0 dB the altitude of the peak in absorption rose to ~100 km, indicating softer precipitation, and the altitude range in which two thirds of absorption occurred decreased slightly to 15 km. Analyses of incoherent scatter radar electron density profiles [*Hargreaves*, 1980; *Hargreaves and Devlin*, 1990] showed that during auroral zone electron precipitation events, the peak in absorption ranges between altitudes of 87 km and 95 km and the half-power 'thickness' of the absorption layer varies from 12 km to 20 km. For the event shown in Figure 4, absorption was weak (~0.13 dB) which

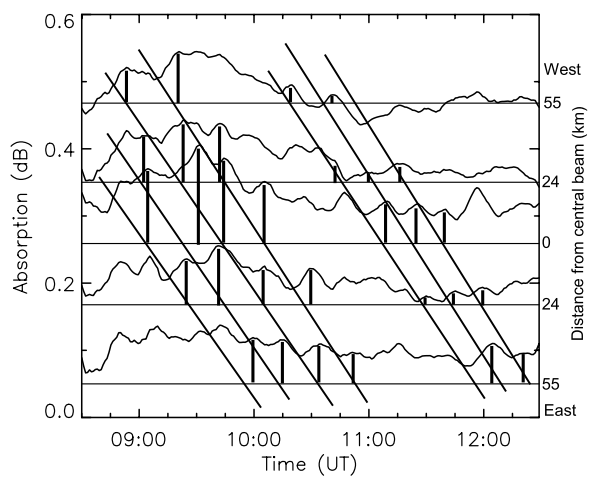

Figure 4. A stacked plot of absorption observed in the five imaging riometer beams shaded in Figure 1 between 08.30 U.T. and 12.30 U.T. on 7 June 2000. That from the eastmost beam is at the bottom of the plot through to that from the westmost beam at the top of the plot. Each signature is offset by 0.1 dB from its neighbours for clarity. Horizontal baselines for each beam are spaced relative to the beam spacings (see text). Selected absorption peaks are indicated by thick vertical lines which originate as time markers on the appropriate baseline. Gradient lines fitted to those time marks at the baselines indicate eastward propagation of the phase fronts.

indicates a likely peak altitude of ~97 km and layer thickness of ~16 km.

[14] The separation at 97 km altitude between the centres of the central and immediately adjacent beams in the central east-west line is 24 ± 1 km; the distance to the next most eastward and westward beams from the central beam is 55 ± 1 km. In Figure 4 a horizontal axis or 'baseline' is marked for each beam. These baselines occur at an arbitrary absorption value but are spaced along the y-axis proportionately to the physical distance between the beam centres when projected onto the D-region ionosphere at 97 km, as annotated on the right axis. Thus, if an event travelling across the beams at a constant velocity is marked on the appropriate baseline as it crosses the centre of that beam, the five resulting time marks (one on each baseline) will fall on a straight line which has a gradient representing the east-west velocity component of the event. The occurrence times of particular peaks in the absorption signature are highlighted by the thick vertical lines which project to the appropriate baseline for that beam. Also shown are gradient fits to those marked times showing the suggested progression of phase fronts which are moving in an eastward direction. Given that the distance across the five beams is 110 ± 2 km, then the mean of these gradients gives an eastward phase velocity for the wave of 19 ± 1 ms^{-1}. The wave period, measured from the autocorrelation of the time series of the central beam is 19.0 ± 0.5 minutes; thus the effective wavelength in the east-west direction is 21.7 ± 1.8 km. On the assumption that the same wave event is being observed with the imaging riometer as is observed in the airglow, then the wave is travelling at a bearing of 70°. Hence the observed wavelength of the absorption signature in the direction of travel is 20.4 ± 1.7 km compared to the estimate of 16 ± 2 km from the airglow image sequence.

[15] The wavelength and wave amplitude observed both by the airglow imager and by the imaging riometer are thus in reasonable agreement. Spectral analysis of the riometer data shows weaker 10.5 and 13.9 minute period peaks in addition to that at 19 minutes. These are closer to the period observed in the imager; the 13.9 minute period, which is visually evident in Figure 4, would give a wavelength of 14.9 km based on the calculations above. It should be noted also that, because the peak sampling altitude of the airglow and absorption are likely to be separated by ~10 km, dissipation of the upward-propagating wave field may lead to differences in wave spectrum at the two altitudes. With typical gravity wave vertical wavelengths ranging between 10 and 50 km, the imaging riometer will be less sensitive than the airglow imager to waves with the shortest vertical wavelengths because the airglow layer is narrower (9 ± 3 km) than the absorption layer (~15 km). Conversely, the fact that the airglow and absorption sampling layers are each several kilometres thick means that there will be considerable overlap between the two samples.

5. Summary

[16] Good agreement is found between mesospheric gravity wave signatures observed using a co-located imaging riometer and airglow imager. This study demonstrates the possibility for riometer usage for gravity wave studies; an in-depth comparison study is planned to determine how often and what scale size waves are evident in both systems. Imaging riometers have considerable advantage over optical instrumentation in that they can be used 24-hours day and night independent of cloud cover and moon light. Like airglow imagers they will be subject to auroral contamination. They have poorer spatial resolution but excellent temporal resolution.

[17] **Acknowledgments.** The dedication of the overwintering personnel at Halley Research Station, Antarctica is gratefully acknowledged. The airglow imager and the imaging riometer are jointly supported by the U.K. Natural Environment Research Council (NERC) and by the U.S. Office of Polar Programs grants OPP-9816465 and OPP-0003881.

References

Baker, D. J., and A. T. Stair, Rocket measurements of the altitude distributions of the hydroxyl airglow, *Phys. Scripta*, *37*, 611–622, 1988.

Detrick, D. L., and T. J. Rosenberg, A phased-array radiowave imager for studies of cosmic noise absorption, *Radio Sci.*, *25*, 325–338, 1990.

Fraser, G. J., The 5-day wave and ionospheric absorption, *J. Atmos. Terr. Phys.*, *39*, 121–124, 1977.

Friedrich, M., and K. M. Torkar, High-latitude plasma densities and their relation to riometer absorption, *J. Atmos. Terr. Phys.*, *45*, 127–135, 1983.

Fritts, D. C., and R. A. Vincent, Mesospheric momentum flux studies at Adelaide, Australia: Observations and gravity wave tidal interaction model, *J. Atmos. Terr. Phys.*, *44*, 605–619, 1987.

Hargreaves, J. K., D-region electron densities observed by incoherent-scatter radar during auroral-absorption spike events, *J. Atmos. Terr. Phys.*, *42, 783–789, 1980.*

Hargreaves, J. K., and T. Devlin, Morning sector electron precipitation events observed by incoherent scatter radar, *J. Atmos. Terr. Phys.*, *52*, 193–203, 1990.

Hickey, M. P., and J. M. C. Plane, A chemical-dynamic model of wave-driven sodium fluctuations, *Geophys. Res. Lett.*, *22*, 2861–2864, 1995.

Krishnaswamy, S., D. L. Detrick, and T. J. Rosenberg, The inflection point method of determining riometer quiet day curves, *Radio Sci.*, *20*, 123–136, 1985.

Lindzen, R. S., Turbulence and stress owing to gravity-wave and tidal breakdown, *J. Geophys. Res.*, *86*, 9707–9714, 1981.

Rose, M. C., M. J. Jarvis, M. A. Clilverd, D. J. Maxfield, and T. J. Rosenberg, The effect of snow accumulation on imaging riometer performance, *Radio Sci.*, *35*, 1143–1153, 2000.

Stauning, P., Ionospheric investigations using imaging-riometer observations, in *Review of Radio Sci. 1993–1996*, edited by W. R. Stone, pp. 157–161, Oxford Univ. Press, Oxford, England, 1996.

Swenson, G. R., and C. S. Gardner, Analytical models for the responses of the mesospheric OH* and Na layers to atmospheric gravity waves, *J. Geophys. Res.*, *103*, 6271–6294, 1998.

Taylor, M. J., M. B. Bishop, and V. Taylor, All-sky measurements of short period waves imaged in the OI (557.7 nm), Na(589.2) and near infrared OH and O_2(0, 1) nightglow emissions during the ALOHA-93 campaign, *Geophys. Res. Lett.*, *22*, 2833–2836, 1995.

Walterscheid, R. L., Gravity wave transports and their effects on the large-scale circulation of the upper mesosphere and lower thermosphere, *Adv. Space Res.*, *27*, 1713–1721, 2001.

R. E. Hibbins and M. J. Jarvis, British Antarctic Survey, Madingley Road, Cambridge CB3 0ET, United Kingdom. (rehi@bas.ac.uk; mjja@bas.ac.uk)

T. J. Rosenberg, Institute for Physical Science and Technology, University of Maryland, College Park, MD 20742, USA. (rosenberg@uarc.umd.edu)

M. J. Taylor, Center for Atmospheric and Space Sciences, Utah State University, Logan, UT 84322, USA. (Mike.Taylor@sdl.usu.edu)